Search for superconductivity in LiBC at high pressure: Diamond anvil cell experiments and first-principles calculations

A. Lazicki,[1,2] C.-S. Yoo,[1] H. Cynn,[1] W. J. Evans,[1] W. E. Pickett,[2] J. Olamit,[2] Kai Liu,[2] and Y. Ohishi[3]
[1]*Lawrence Livermore National Laboratory, Livermore, California 94550, USA*
[2]*Physics Department, University of California, Davis, California 95616, USA*
[3]*SPring-8/JASRI, Hyogo 679-5198, Japan*
(Received 16 November 2006; published 9 February 2007)

Diamond anvil cell experiments augmented by first principles calculations have been used to investigate the behavior at high pressure of lithium borocarbide (LiBC), which is structurally and electronically similar to the superconductor MgB_2. It is found to remain stable up to 60 GPa with no crystal structure change and without a previously reported lattice parameter anomaly. Large anisotropy in the linear compressibility of the layered hexagonal structure is identified and related to the distinctly different bonding types within and between the hexagonal planes; a mixture of covalent and ionic intralayer bonding and interlayer bonding consisting of van der Waals–type interactions and weak (but increasing under pressure) covalency. Metallization is not found until a calculated pressure of at least 345 GPa, and pressure removes the similarity in electronic structure between LiBC and MgB_2; reducing the cell volume causes an increase in the σ and π electronic band gaps. Metallization is finally an indirect gap closure and the holes do not go into any sigma bands, ruling out the possibility of a new MgB_2-type high-pressure superconductor.

DOI: 10.1103/PhysRevB.75.054507 PACS number(s): 62.50.+p, 74.62.Fj, 64.30.+t

I. INTRODUCTION

The discovery of high-T_c (40 K) superconductivity in metal diboride MgB_2 (Ref. 1) has led to an extensive search for similar behavior among related intermetallic compounds. Lithium borocarbide (LiBC) is isovalent with and structurally similar to MgB_2, with hexagonal sheets of BC in place of B_2 and Li in place of Mg (Fig. 1).[2] However, due to the alternation of B and C atoms within and perpendicular to the hexagonal sheets, LiBC is an insulator.[3] If it can be driven metallic, such as by hole doping, suggestions of superconductivity to temperatures even higher than MgB_2 have been made,[4] and verified by calculations of electron-phonon coupling strength.[5,6] However, no experimental efforts to date have reported superconductivity above 2 K in this compound,[3,7–11] and additional theoretical studies have attempted to further illuminate the behavior of LiBC.[3,6,12,13]An investigation of lattice dynamics of Li_xBC at various annealing temperatures has shown that standard hole-doping techniques may remove only small amounts of surface Li—insufficient for superconductivity.[10] Resonant inelastic x-ray scattering experiments have been interpreted in terms of lack of complete hybridization between B and C states, indicating that electronic structure calculations may inadequately describe this material since they do not take into account this effect, or such effects as B-C disorder and structural relaxation near hole dopants.[14]

Although high-T_c superconductivity in Li_xBC continues to elude us, over the course of the previous investigations several other interesting properties of LiBC have been suggested, including extreme anisotropy in the thermal expansion[3] and Born effective charges,[15] and calculated anomalous behavior of the *c*-axis lattice constant under pressure which implies a sort of negative Poisson ratio.[12]

As an alternative to hole doping, another possibility for producing an insulator-metal transition and possible superconductivity is by applying pressure. In this paper we pursue this possibility both with experiment and theory calculations, and we investigate trends and changes in structural and bonding anisotropy under pressure, including the predicted lattice parameter anomaly.[12]

II. HIGH PRESSURE EXPERIMENTS

The synthesis of LiBC has been reported before[8] and is summarized here. Amorphous boron (99.99%, 325 mesh, Alfa Aesar) and carbon (99.9999%, 200 mesh, Alfa Aesar)

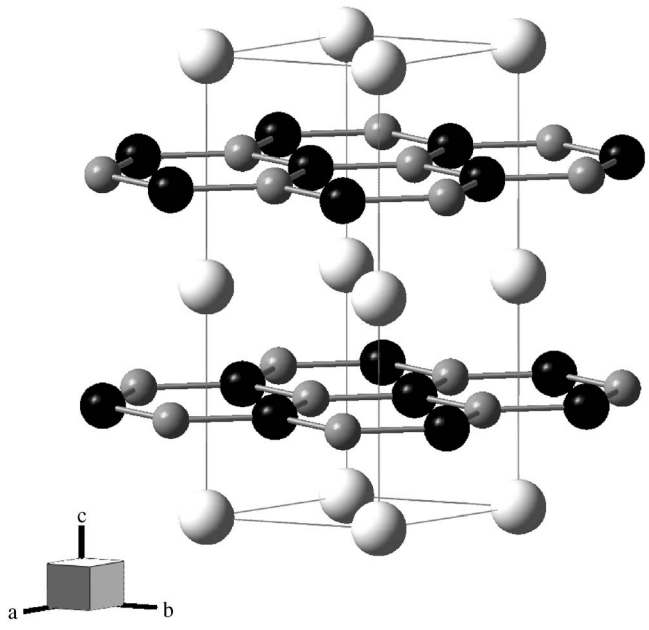

FIG. 1. LiBC crystal structure. White, black, and grey atoms represent lithium, carbon, and boron, respectively.

powders were thoroughly mixed in a 1:1 atomic ratio for ~45 min. Lithium (99.9%, ingot, Alfa Aesar) was added to the boron-carbon mixture in a 1.2:1:1 (Li:B:C) atomic ratio in an argon-filled dry box. The elements were mixed together for ~2 h with a mortar and pestle, resulting in a uniform black powder which was then pressed at ~0.4 GPa into a 6 mm diameter pellet. This pellet was placed in an argon-filled arc furnace. The argon was first purified by arc melting a zirconium pellet. The $Li_{1.2}BC$ pellet was arc melted, starting a self-sustaining exothermic reaction where the excess lithium (having served as a flux) was released, resulting in a golden LiBC pellet.

Pieces of LiBC cut from the arc-melted pellet were loaded into a membrane diamond anvil cell (DAC) of Livermore design. Brilliant cut diamonds with 0.3 mm flats were used with a 0.15 mm diameter sample chamber in a rhenium gasket of 0.05 mm initial thickness to achieve a pressure range of 1 to 60 GPa. No pressure medium was used in the experiments, as the reactivity of LiBC is uncertain. Copper was included in the sample chamber as an internal pressure indicator. All sample loadings were performed in an inert environment, as LiBC is hygroscopic.

High-pressure behavior of LiBC was investigated by angle dispersive x-ray diffraction (ADXD) at ambient temperature at the microdiffraction beamline BL10XU of the SPring-8 facility. In these experiments, we used intense monochromatic x rays ($\lambda = 0.4168$ Å) microfocused to about 0.02 mm at the sample. The x-ray diffraction patterns were recorded on a high-resolution image plate detector (Rigaku R-AXIS IV) and x-ray charge-coupled device (Bruker APEX). The recorded two-dimensional diffraction images (Debye-Scherrer rings) were then integrated to produce high quality ADXD patterns using FIT2D and analyzed with the XRDA (Ref. 16) and GSAS (EXPGUI) (Ref. 17) programs.

III. THEORETICAL CALCULATIONS

We performed electronic structure calculations using the mixed basis set of augmented plane waves + local orbitals and linearized augmented plane waves as implemented in WIEN2k code.[18] A gradient corrected Perdew-Berke-Ernzerhof functional[19] [generalized gradient approximation (GGA)] to density functional theory was used to describe the exchange and correlation effects. Muffin tin radii (R_{mt}) were set so that neighboring muffin tin spheres were nearly touching at each volume, and the plane wave cutoff K_{max} was determined by $R_{mt}K_{max}=9.0$. The Brillouin zone was sampled on a uniform mesh with 280 irreducible k points. The energy convergence criterion was set to 0.1 mRy.

IV. EXPERIMENTAL RESULTS

The LiBC crystal structure shown in Fig. 1 (first determined by Wörle *et al.*[2]) was confirmed from a Rietveld refinement of the ADXD spectra. A sample refinement at 4.5 GPa is shown in Fig. 2. The compound takes on D_{6h}^4 ($P6_3/mmc$) space group symmetry with Li, B, and C atoms in 2a, 2c, and 2d Wyckoff positions, respectively. The B and C atoms alternately occupy the sites within graphenelike

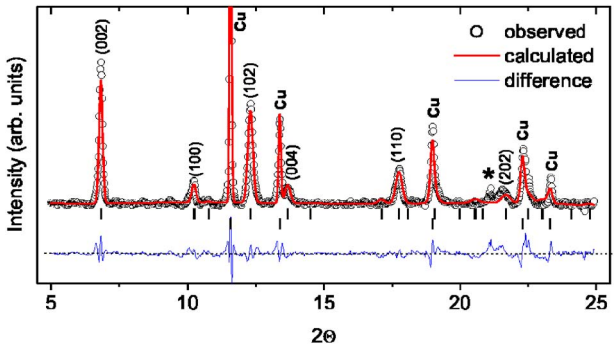

FIG. 2. (Color online) Sample GSAS refined ADXD pattern for LiBC and Cu at ~4.5 GPa. Major LiBC peaks are labeled with their *hkl* indices. The small peak labeled with an * near $2\Theta = 21°$ does not originate from the sample.

hexagonal sheets, and Li ions fill the interlayer regions. The unit cell along the c axis is doubled, because of the alternating stacking of the BC layers, with B superposed directly above C. The compound was found to remain stable in the ambient pressure phase up to 60 GPa, which was the maximum pressure achieved in the experiment. Experimental pressure-volume data are shown in Fig. 3, and fit with the third order Birch-Murnaghan equation of state:

$$P = \frac{3}{2}B_0(v^{-7/3} - v^{-5/3})\left[1 + \frac{3}{4}(B_0' - 4)(v^{-2/3} - 1)\right], \quad (1)$$

where $v = V/V_0$. Fitting parameters are $V_0 = 45.62(7)$ Å^3 per unit cell, $B_0 = 125(3)$ GPa, and $B' = 3.7(1)$. The equation of state was also calculated from first principles and the results are shown as the dotted curve in Fig. 3, with equation of state fitting parameters $V_0 = 46.04(5)$ Å^3, $B_0 = 123(2)$ GPa,

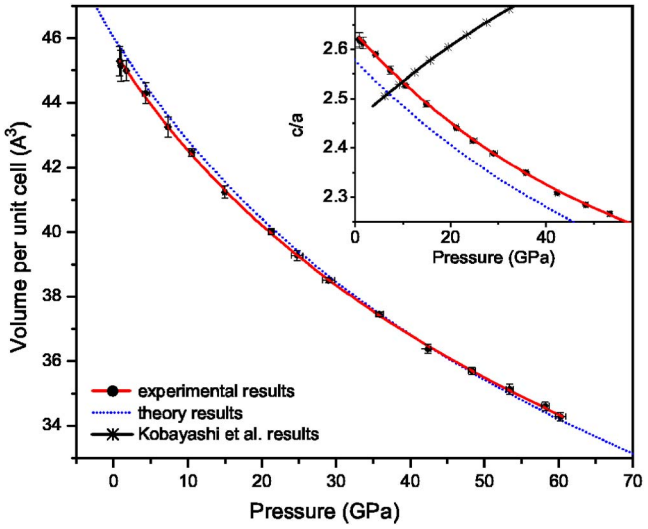

FIG. 3. (Color online) Equation of state of LiBC up to 60 GPa. The solid line is a third-order Birch-Murnaghan fit to the experimental data, and the dotted line represents the calculated theoretical equation of state. In the inset, results from this study are compared with those of Kobayashi *et al.* (Ref. 12) for the evolution of c/a with pressure.

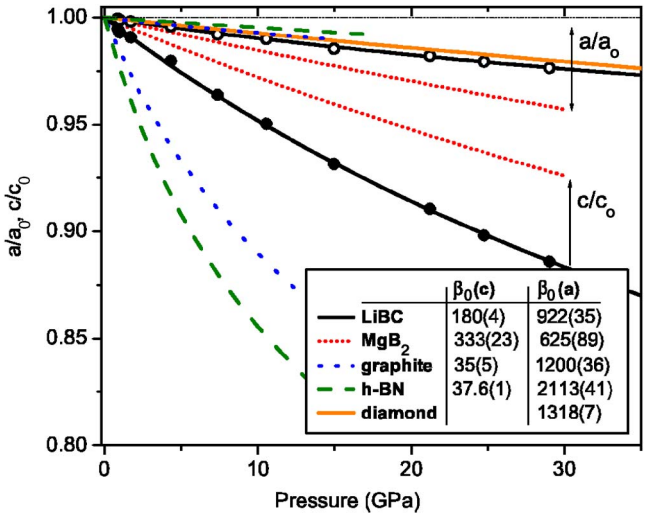

FIG. 4. (Color online) High pressure behavior of a and c lattice parameters (normalized to ambient pressure a_0 and c_0), compared with MgB_2 and similar layered hexagonal compounds (Ref. 21–23) as well as with diamond (Ref. 24). Curves shown are the first-order Murnaghan equation [Eq. (2)] fits to experimental data (circles). Values for first order axial compression coefficients (as described in the text) are shown in the inset for LiBC and related compounds (Ref. 21–24). β_0^{-1} is the linear compressibility at zero pressure.

and $B'=3.43(9)$. Agreement between experiment and theory for LiBC is remarkably good. The bulk modulus of this material is of the same order as that of MgB_2 and other AlB_2-type compounds, which range from 105 to 193 GPa.[4] The compressibility is moderate, but the good agreement between calculations (for which fully hydrostatic compression is enforced) and experiment indicates that, although no pressure medium was used in the experiment, conditions in the DAC sample chamber appear quasihydrostatic.

The evolution of the c/a lattice parameter ratio is shown in the inset of Fig. 3, compared with the calculations of Kobayashi and Arai[12] (with the volume values quoted in[12] transformed to pressures using the equation of state obtained in this study). Using all-electron calculations of precisely the same sort also employed here, they find that the c/a ratio actually increases as volume is reduced. The reason for the significant disparity between the results of this work and those presented in Ref. 12 is unclear, but it appears to significantly undermine their conclusions. They claim that this unexpected c/a increase with pressure gives further evidence for an anomalous c-axis contraction under anisotropic $a-b$ compression (implying a negative Poisson ratio), which was obtained by first-principles molecular dynamics calculations.

The linear compressibility of LiBC is compared with a variety of other low-Z layered hexagonal materials, including MgB_2, by fitting normalized lattice parameters as a function of pressure with the one-dimensional analog to the first order Murnaghan equation[20]

$$r/r_0 = [(\beta'/\beta_0)P + 1]^{-1/\beta'}. \quad (2)$$

This procedure provides a very approximate description of the nonlinear relation between lattice parameters and pressure. Curves are shown in Fig. 4, and β_0 fitting parameters (relative rather than exact numerical values should be taken as physically meaningful) are summarized in the inset. Ambient pressure lattice parameters were not measured experimentally for LiBC since the diamond anvil cell was loaded at ~0.8 GPa, and so these values were taken from the fitting with Eq. (2), yielding $a_0=2.7141(7)$ Å and $c_0=7.146(5)$ Å.

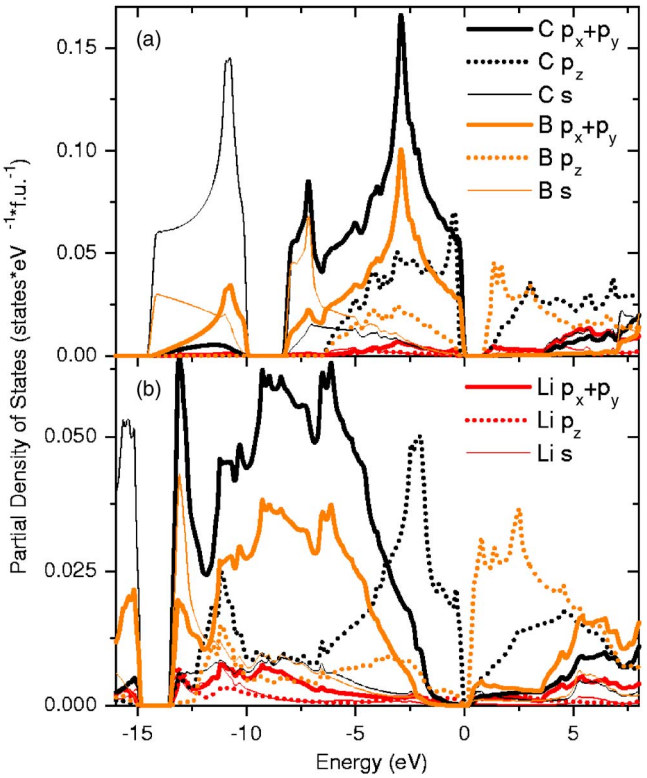

FIG. 5. (Color online) Projected density of states (a) at ambient pressure and (b) at metallization.

The a-axis compressibility of LiBC is shown to be quite close to that of diamond and graphite a-axis compressibilities, confirming the existence of strong covalent bonds within the hexagonal BC planes. LiBC is over five times more compressible along the c axis than along the a axis, indicating much weaker interlayer bonding, similar to the van der Waals–type interactions between neighboring planes in h-BN. The greater stiffness along the c axis of LiBC compared to graphite and h-BN, however, is most likely a result of the presence of Li ions between the planes, just as the larger Mg ions in MgB_2 contribute to an even larger c-axis stiffening.

V. DISCUSSION

The anisotropy in linear compressibility is clearly related to bonding in the material, which we investigate with electronic structure calculations. An examination of the calculated projected density of states in Fig. 5 reveals the hybridized states which form covalent bonds in LiBC. The σ states are formed mainly by bonding combinations of sp^2 states on both B and C, as in graphite. Lee and Pickett find that B and C are very different chemically, however, with Born effective

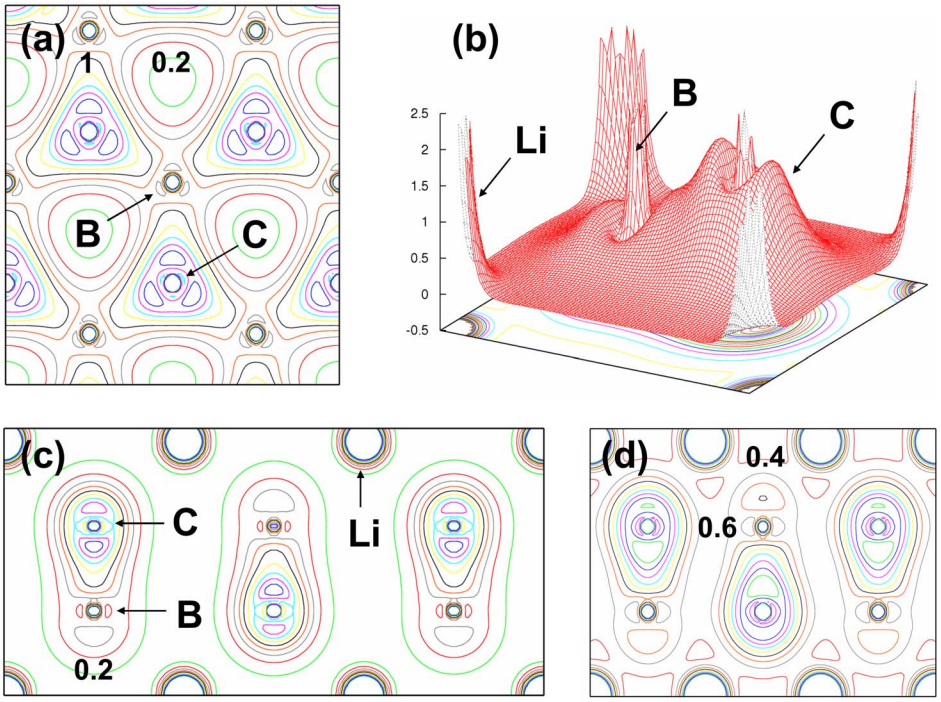

FIG. 6. (Color online) Electron density in (a) the (0001) plane, (b) the $(10\bar{1}0)$ plane, and (c) contours along the $(10\bar{1}0)$ plane at ambient and (d) metallization pressure. Contour values are given in units of $e/\text{Å}^3$. Subsequent contours differ by $0.2e/\text{Å}^3$.

charges of approximately +1, +2, and −3 given for Li, B, and C.[15] Figure 6 shows that the electron density is indeed largely concentrated in the sp^3 orbitals around the carbon atom; the covalent bond is strongly polarized and the atomic interactions are a mixture of covalent and ionic and remain thus up to metallization. Part of the stiffness of the material in the $x-y$ plane is due to Coulomb repulsions between the significantly electronegative C atoms. It is the BC alternation within the plane that is responsible for the gap (at Γ; see Fig. 7) in the σ states; a gap which increases initially as pressure is increased (similar to the gap between bonding and antibonding σ bands in diamond[25]) and remains large up to metallization, with the bonding sigma states remaining fully occupied and dropping further and further below the Fermi level.

The interplanar bonding, as is obvious from the experimentally determined high compressiblity, is much weaker than that which exists within the planes. The lack of electron density in the interstitial regions between the BC planes [Fig. 6(c)], and the small amount of hybridization seen from the projected density of states (Fig. 5) shows that the $B\ p_z$ and $C\ p_z$ states are relatively localized and weakly interacting. The B-C alternation along the c axis is responsible for the gap between the primarily $C\ p_z$ upper valence bands and the $B\ p_z$ conduction bands. As pressure increases, this gap eventually collapses as the BC layers are brought closer together and the bands broaden. Lee and Pickett[15] propose that there is considerable covalency between Li and the BC layers, particularly between Li and C. This effect is not obvious from an examination of the electron density and the projected density of states (Fig. 6), but it appears that this covalency increases with pressure since, at metallization, the valence bands between 0 and −14 eV have acquired very appreciable Li character.

The band structure of LiBC is shown in Fig. 7. At ambient pressure, it bears many similarities to that of MgB_2; they both have nearly flat bands of $p\sigma$ character at the top of the valence bands between Γ and A (which, in MgB_2, cross the Fermi level to form nearly cylindrical Fermi surfaces around the Γ point), as well as bonding and antibonding $p\pi$ bands near the Fermi level (which cross it, to form Fermi surface "webbed tunnels" in the case of MgB_2) near the M and K regions. For MgB_2, these two Fermi surface features are characterized by different superconducting energy gaps, making it a two-band superconductor with a transition temperature of 39 K.[26] The band structure of LiBC was investigated under pressure, to see if any similar features would evolve. As pressure increases, the occupied $p\ \sigma$ bands (which have a mixture of boron and carbon character) drop in energy with respect to the C π bands, losing their flatness between Γ and A and dropping even further below the Fermi level. The gap between the σ and σ^* bands remains large. The unoccupied $p\ \pi$ bands (predominantly from boron) drop in energy at L and H, while increasing between Γ and M and between Γ and K, and finally overlapping to become semimetallic at a calculated pressure of 324 GPa $(V/V_0=0.46)$, which is a lower limit since the GGA approximation tends to cause an underestimate of the band gap. This is an indirect gap closure, and the direct gap near M and K, which is closed in the case of MgB_2, becomes larger under pressure. After metallization, the density of states at the Fermi level increases rather rapidly to 0.1 eV^{-1} by 450 GPa [compared to $N(E_F)$ $\sim 0.7\ \text{eV}^{-1}$ in MgB_2 and $Li_{0.5}BC$ (Ref. 5)], but none of these states come from the σ bands, which are of primary importance for superconductivity in the case of MgB_2. We have not investigated the issue of electron-phonon coupling, but this examination of the electronic behavior alone indicates that we are very unlikely to see LiBC become superconducting under pressure experimentally; indeed (assuming no additional phase transitions), it does not even metallize in a range which is practically achievable using current static high pressure methods.

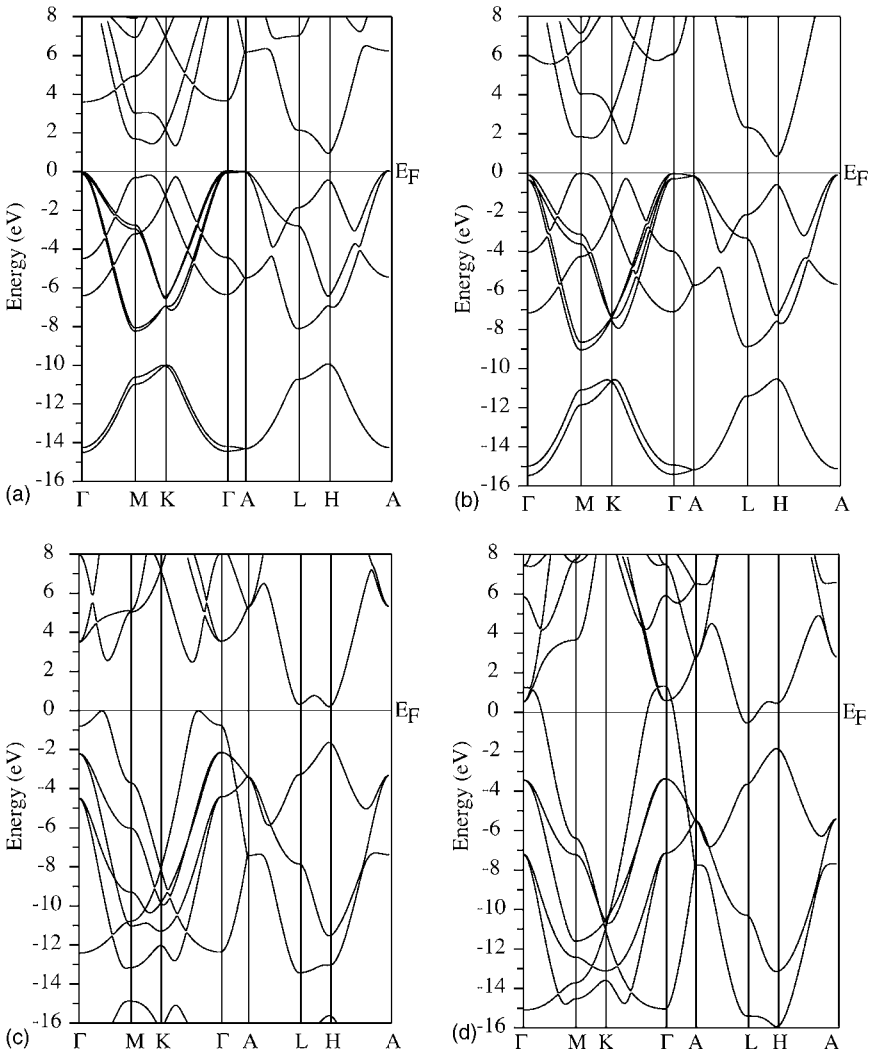

FIG. 7. Band structures (a) at ambient pressure, at (b) ~60 GPa, (c) at ~325 GPa, and (d) at ~450 GPa.

VI. CONCLUSION

LiBC is shown experimentally to remain stable in the ambient pressure crystal structure up to at least 60 GPa. Under quasihydrostatic pressure no anomalous behavior of the lattice parameters was observed; reducing the volume caused a drop in the c/a ratio representing the expected movement towards a more close-packed, isotropic material. The large anisotropy in linear compressibility indicates that the bonding in this material is also highly anisotropic. The strong intralayer bonding—similar to *h*-BN and graphite interlayer interactions—has a mixture of covalent and ionic character. There is very little interaction between neighboring layers, resulting in high compressibility along *c*. Increasing pressure causes increased interlayer interaction, as well as an increase in covalency between Li and neighboring BC planes. Calculations do not predict metallization until over 325 GPa, and by that pressure the electronic structure has become dissimilar to that of MgB_2. Most importantly, the increased gap in the σ bands indicates that, if superconductivity were to appear, it must be of a sort unrelated to the σ states, such as has been observed in graphite intercalate compounds[27] rather than MgB_2.

ACKNOWLEDGMENTS

Work at the SPring-8 BL10XU was performed with the approval of the Japan Synchrotron Radiation Research Institute (JASRI), and has been supported by the LDRD(04ERD020) and SEGRF programs at LLNL, University of California, under DOE Grant No. W7405-ENG-48, by the SSAAP (DE-FG01-06NA2620) and by the Alfred P. Sloan Foundation.

[1] J. Nagamatsu, N. Nakagawa, T. Muranaka, Y. Zenitani, and J. Akimitsu, Nature (London) **410**, 63 (2001).
[2] M. Wörle, R. Nesper, G. Mair, M. Schwarz, and H. G. von Schnering, Z. Anorg. Allg. Chem. **621**, 1153 (1995).
[3] A. M. Fogg, P. R. Chalker, J. B. Claridge, G. R. Darling, and M. J. Rosseinsky, Phys. Rev. B **67**, 245106 (2003); A. M. Fogg, J. Meldrum, G. R. Darling, J. B. Claridge, and M. J. Rosseinsky, J. Am. Chem. Soc. **128**, 10043 (2003).
[4] P. Ravindran, P. Vajeeston, R. Vidya, A. Kjekshus, and H. Fjellvåg, Phys. Rev. B **64**, 224509 (2001).
[5] H. Rosner, A. Kitaigorodsky, and W. E. Pickett, Phys. Rev. Lett. **88**, 127001 (2002).
[6] J. K. Dewhurst, S. Sharma, C. Ambrosch-Draxl, and B. Johansson, Phys. Rev. B **68**, 020504(R) (2003).
[7] Y. Nakamori and S. I. Orimo, J. Alloys Compd. **370**, L7 (2004).
[8] L. Zhao, P. Klavins, and Kai Liu, J. Appl. Phys. **93**, 8653 (2003).
[9] A. Bharathi, S. J. Balaselvi, M. Premila, T. N. Sairam, G. L. N. Reddy, C. S. Sundar, and Y. Hariharan, Solid State Commun. **124**, 423 (2002).
[10] B. Renker, H. Schober, P. Adelmann, P. Schweiss, K.-P. Bohnen, and R. Heid, Phys. Rev. B **69**, 052506 (2004).
[11] D. Souptel, Z. Hossain, G. Belu, W. Löser, and C. Geibel, Solid State Commun. **125**, 17 (2003).
[12] K. Kobayashi and M. Arai, Physica C **388-389**, 201 (2003); J. Phys. Soc. Jpn. **72**, 217 (2003).
[13] S. Lebegue, B. Arnaud, P. Rabiller, M. Alouani, and W. E. Pickett, Europhys. Lett. **68**, 864 (2004); **69**, 311 (2005).
[14] P. F. Karimov, N. A. Skorikov, E. Z. Kurmaev, L. D. Finkelstein, S. Leitch, J. MacNaughton, A. Moewes, and T. Mori, J. Phys.: Condens. Matter **16**, 5137 (2004).
[15] K.-W. Lee and W. E. Pickett, Phys. Rev. B **68**, 085308 (2003).
[16] S. Desgreniers and K. Lagarec, J. Appl. Crystallogr. **31**, 109 (1998).
[17] B. H. Toby, J. Appl. Crystallogr. **34**, 210 (2001).
[18] P. Blaha, K. Schwarz, G. K. H. Madsen, D. Kvasnicka, and J. Luitz, Computer code WIEN2K, An Augmented Plane Wave + Local Orbitals Program for Calculating Crystal Properties, Karlheinz Schwarz, Techn. Universität Wien, Wien, 2001.
[19] J. P. Perdew, K. Burke, and M. Ernzerhof, Phys. Rev. Lett. **77**, 3865 (1996).
[20] F. D. Murnaghan, Proc. Natl. Acad. Sci. U.S.A. **30**, 244 (1944).
[21] A. F. Goncharov, V. V. Struzhkin, E. Gregoryanz, J. Hu, R. J. Hemley, H. K. Mao, G. Lapertot, S. L. Bud'ko, and P. C. Canfield, Phys. Rev. B **64**, 100509(R) (2001).
[22] Y. X. Zhao and I. L. Spain, Phys. Rev. B **40**, 993 (1989).
[23] V. L. Solozhenko, G. Will, and F. Elf, Solid State Commun. **96**, 1 (1995).
[24] F. Occelli, P. Loubeyre, and R. Letoullec, Nat. Mater. **2**, 151 (2003).
[25] M. P. Surh, S. G. Louie, and M. L. Cohen, Phys. Rev. B **45**, 8239 (1992).
[26] H. J. Choi, D. Roundy, H. Sun, M. L. Cohen, and S. G. Louie, Nature (London) **418**, 758 (2002).
[27] G. Csányi, P. B. Littlewood, A. H. Nevidomskyy, C. J. Pickard, and B. D. Simons, Nat. Phys. **1**, 42 (2005).